 ISBN: 978-1-926872-32-2

INVESTIGATION OF FILIFORM CORROSION ON PAINTED 6000-SERIES ALUMINUM ALLOYS

*N. Hosking[1] and M. Nichols[1]

[1]Ford Motor Company Ltd.
PO Box 2053
MD 3182 RIC
Dearborn, MI 48121
(*Corresponding author: nhoskin5@ford.com)

ABSTRACT

Aluminum alloys are increasingly used for automotive body construction but are susceptible to filiform corrosion or paint blistering in service. Filiform corrosion resistance of two 6000-series aluminum alloys was investigated in this work. Test panels were produced with full automotive coating layers and scribed parallel and perpendicular to the rolling direction. The corrosion exposure comprised an inoculation step with acidified salt solution followed by a 6-week exposure period at 95% relative humidity and either 25°C or 70°C. Greatest corrosion activity was measured on the alloy with higher copper content, AA6111. Higher temperature exposure led to greatly enhanced corrosion activity for AA6111 compared to the lower temperature exposure. The 70°C exposure also led to greater mean corrosion-affected area measurements for the low copper aluminum alloy, AA6022, but the effect was not as stark as that observed for AA6111. Rolling direction affected the propagation direction, and possibly mechanism, of the corrosion effects. Cross-sectional analysis revealed dense corrosion products within the filament, comprising mostly aluminum and oxygen but with traces of chloride and sulphate. Development of varying filament and blister types on a single test panel and the progression of corrosion underneath a filament into the substrate indicate that several corrosion mechanisms can develop on the test panel, testament to the complexity of the corroding surface developed on an aluminum automotive body panel.

KEYWORDS

Corrosion, aluminum alloys, filiform, blistering

 ISBN: 978-1-926872-32-2

INTRODUCTION

Use of aluminum alloys as a construction material for automotive bodies is increasing due to more stringent requirements on fuel economy performance. However, painted aluminum alloy automotive body panels may be subject to cosmetic corrosion, whereby corrosion activity occurs underneath the painted surface and leads to unsightly blistering or filiform-type defects of the paint layer (Bovard, 2010; LeBozec, Persson, & Thierry, 2004; McMurray, Holder, Williams, Scamans, & Coleman, 2010). The aluminum alloy surface of a painted automotive body panel is the output of a series of processes that tend to promote heterogeneity of the material. There is an extensive literature available on the characteristics of unpainted aluminum alloy surfaces and how these characteristics affect localized corrosion. It is a reasonable extension to consider that the alloy surface underneath the paint layers retains characteristics and behaviors of the unpainted alloy surface, and indeed there are reports relating these surface characteristics to coated material corrosion resistance, see for example Bautista's (1996) review. These coated panels generally tend to be laboratory representations, for example e-coated only samples (Olivier, Poelman, Demuynck, & Petitjean, 2005), single-layer coatings (McMurray et al., 2010) or transparent coatings (Jenkins & Armstrong, 1996), as required by the researchers to generate useful experimental results within a reasonable time period. There are rather fewer reports in the public domain that attempt to relate cosmetic corrosion performance of fully-painted test panels representative of the existing automotive plant processes to the underlying substrate condition. Painted test panels used in this work were of plant-quality standards with the intention to relate scribe creep performance to the known or assumed characteristics of the uncoated material and to the characteristics of the paint layers.

Localized Corrosion of Aluminum Materials

The naturally-formed oxide present on the surface of aluminum passivates the material surface (Kaesche, 1978) and leads to generally very low rates of corrosion for aluminum panels compared to, for example, steel panels. Pure aluminum has been shown to develop localized corrosion due to heterogeneities in the material surface (Davoodi, Pan, Leygraf, & Norgren, 2008), with corrosion progressing along closely-packed planes of crystallographic structures. The addition of alloying elements to the aluminum matrix leads to increased heterogeneity compared to the unalloyed material, and it is not surprising that increased localized corrosion for aluminum alloys compared to pure aluminum is widely reported in the literature. Alloying elements lead to a complex microstructure, featuring the precipitation of intermetallic phases, (IMPs). Localized corrosion is associated with the presence of IMPs and changes in microstructure at and near the grain boundaries, when the material is exposed to the corrosive environment.

The increase of localized corrosion by the alloying elements is explained by the potential difference that exists between certain IMPs, grain boundaries and the aluminum matrix (Davoodi et al., 2008; Liang, Rometsch, Cao, & Birbilis, 2013; Szklarska-Smialowska, 1999). More noble sites, such as copper- or iron-rich IMPs, act as micro-cathodes, promoting corrosion of adjacent less noble sites, such as the aluminum matrix or copper / iron-depleted grain boundaries or magnesium-rich IMPs. Skzlarsaka-Smialowska's (1999) extensive review of aluminum pitting corrosion concluded that copper-rich and iron-rich IMPs are those that significantly decrease the resistance of an aluminum alloy to localised corrosion. Liang et al.'s (2013) study of 6000-series aluminum alloys noted that the magnitudes of copper and magnesium additions to the alloy were significant factors in the promotion of localized corrosion of the alloy substrate, with the presence of copper being a stronger promoter of localized corrosion than the presence of magnesium. Liu (2007) reported that the IMPs tended to align with the rolling direction.

Mechanical grinding or sandblasting the aluminum surface has been reported to increase the material's susceptibility to localized corrosion (Bautista, 1996; McMurray et al., 2010). This observation has been extended to the more general case of a "near surface-deformed layer", NSDL, which, according to Eckermann et al. (2008) may

 ISBN: 978-1-926872-32-2

be produced by any shearing event applied to the aluminum surface. The properties of the NSDL have been shown to be different from the underlying bulk material (Afseth, Nordlien, Scamans, & Nisancioglu, 2002; Bovard, 2010; Y. Liu et al., 2007; McMurray et al., 2010) and as filiform corrosion takes place at this surface, it is the nature of this layer that is significant for the subsequent cosmetic corrosion resistance of the final automotive panel. Afseth et al. (2002) characterized the surface layer for AA3005 material and reported greater density of fine, secondary precipitates and a reduced density of IMPs in the surface compared to the bulk, indicating a further complexity of the aluminum alloy, being heterogeneous not just across the surface but also through the thickness. McMurray et al. (2010) described the NSDL for abraded AA6111 alloy as being approximately 2µm thick

Heat-treatment of 6000-series aluminum alloys results in the diffusion and precipitation of IMPs out of solution, which both enhances the materials' mechanical properties through what is known as precipitation strengthening, and leads to localized depletion of IMPs along the grain boundaries, giving rise to a particulate free zone, PFZ, (Guillaumin & Mankowski, 2000; Liang et al., 2013). Increased number and density of IMPs, and consequently PFZs, lead to increased heterogeneity of the material surface, with greater frequency of cathodic and anodic micro-sites, and thereby increased susceptibility to localized corrosion.

Filiform Corrosion of Painted Aluminum Substrates

It is now generally accepted that the mechanism of filiform corrosion on painted aluminum substrates is anodic undermining at the filiform "head" with a trailing cathodic tail (Delplancke et al., 2001; LeBozec et al., 2004). Filiform corrosion or paint blistering can be considered as localized failures in the paint to substrate adhesion and so the response of the paint system applied to the aluminum substrate is critical to the finished panel performance. The initial stages of the paint shop pre-treatment line consist of aqueous degreasing and cleaning stations that remove oil and oxides from the panels and activate the surfaces for deposition of e-coat. The pre-treatment applied to the aluminum substrate acts as the substrate to paint layers interface. The standard automotive pre-treatment is a zinc-phosphate system, including nickel and/or manganese additions (Ogle, Tomandl, Meddahi, & Wolpers, 2004) and typically enhanced by a secondary zirconium-based passivation step. Investigation of the stability of the phosphate layer on galvanized steel substrates has shown that the phosphate layer may dissolve in alkaline solutions, with increased dissolution of monocationic type phosphate crystals compared to tricationic crystals (Jiang, Wolpers, Volovitch, & Ogle, 2012). E-coat and paint layers are applied on top of the zinc-phosphate conversion-coated aluminum substrates.

The surface activation and the conversion coating steps do not resolve the surface heterogeneities present on the incoming substrate – indeed the chemical and electrochemical pre-treatments naturally proceed in a heterogeneous manner for a heterogeneous substrate (Sun et al., 2002), resulting in a layer of varying thickness across the surface (Susac et al., 2004). Jenkins and Armstrong (1996) reported reduced filiform corrosion for painted substrates with a rougher surface compared to similarly painted substrates with a smooth substrate and attributed this difference to improved coating adhesion for the rougher substrate. Bautista's (1996) review supported the idea that poor adherence of coating to substrate led to increased filiform corrosion but, interestingly, related poor adhesion to rough surfaces, rather than smooth surfaces. Presumably Bautista's (1996) notion of a rough surface was more akin to the mechanically-abraded surfaces described by Bovard et al. (2010) and Eckermann et al. (2008). It can be understood that a heterogeneous interface, in terms of both coverage and thickness of zinc phosphate coating and in the electrochemical nature of the underlying aluminum alloy surface, is likely to be more susceptible to filiform corrosion, or perhaps under some conditions, paint delamination or blistering.

Blistering on Painted Substrates

Blisters have been defined as local defects in the coating due to distension of the coating that occurs concomitantly with a loss of adhesion at the metal to coating interface of between coating layers (Prosek et al., 2010). Such loss of adhesion has been anecdotally observed to be more severe on alloys that are coated with a

 ISBN: 978-1-926872-32-2

complete paint system as opposed to only pretreatment and E-coat. The additional paint layers lead to higher stresses in the coating system, particularly at elevated temperatures and high humidity levels due to the thermal and moisture expansion mismatch between the coatings and the substrates (Nichols & Darr, 1998; Perera & Vanden Eynde, 1987). A study of paint blistering noted that local de-adhesion of the coating is a first step in the blistering process (Prosek, Nazarov, Stoulil, & Thierry, 2012). The authors found that the rate of water uptake in the coating did not have a significant effect on paint blistering, similar to an earlier report by Delplancke et al. (2001). Blistering initiation was attributed to the local loss of metal-coating adhesion due to hydrolysis of interfacial bonds. Exposure of such areas to elevated temperatures resulted in paint buckling, considered to be due to compressive stress arising from paint swelling and expansion at elevated temperature and humidity. Perera and Vanden Eynde (1987) reported that stresses in coatings arise mostly below the glass transition temperature, T_g, and that the T_g value decreases with increased RH.

Nichols and Darr (1998) studied multi-layer automotive coatings and reported that swelling and plasticization of a coating may be caused by changes in the humidity of the environment. The authors highlighted the relatively low fracture energy of the clearcoat layer of the automotive paint system compared to the other paint layers. Environmental exposure, such as via weathering tests, lower the fracture energy further such that film-forming and hygrothermal stresses within the paint system may lead to cracking of the clearcoat layer.

EXPERIMENTAL

Materials

Two different aluminum alloys, AA6111 and AA6022, were used in this work. Chemical analysis of each alloy type was conducted using a SpectroMax optical emission spectrometer (Simões, Battocchi, Tallman, & Bierwagen). Four sparks were applied to a coupon specimen for each material and the average weight percentage, (wt.%), of each element of interest is presented in table 1. It can be seen that AA6111 contains significantly higher amounts of copper than AA6022.

Table 1 – OES chemical analysis (wt.%) of alloying elements in AA6111 and AA6022

Alloy	Si	Fe	Cu	Mn	Mg	Cr	Ni	Zn	Ti
AA6111	0.831	0.242	0.543	0.161	0.625	0.009	0.006	0.039	0.055
AA6022	0.840	0.191	0.110	0.085	0.586	0.034	0.005	0.005	0.023

Rolling direction for each panel was noted so that scribes could be cut parallel and perpendicular to the rolling direction. Both alloys were in a naturally-aged condition prior to test panel fabrication. These alloys are bake-hardening, responding to the heat exposure in the automotive e-coat ovens. The test panels were processed through the pre-treatment line at an automotive paint facility. The pre-treatment comprised of cleaning, immersion zinc-phosphate, immersion passivation and standard automotive e-coat stages. The e-coat was cured for 30 minutes at 180°C. Full paint layers were applied in the laboratory using standard automotive paint, comprising primer, base-coat and clearcoat layers, yielding a total coating thickness of approximately 120µm on the aluminum alloy surface. The approximate thickness of each coating layer is given in table 2.

Table 2 – Thickness of each coating layer applied to the substrates

	E-coat	Primer	Basecoat	Clearcoat
Thickness (µm)	15	30	20	55

 ISBN: 978-1-926872-32-2

Exposure

Eight test panels were prepared for each substrate. The painted panels were scribed to base metal using a hand-held scribing tool with carbide tip. Scribes were approximately 30mm long and 0.5mm wide. The rolling direction was referred to the longer edge of the test panels and scribes were cut parallel (panels labelled transverse) and perpendicular (panels labelled longitudinal) to the rolling direction for half of the test panels. The scribed panels were immersed for 4 minutes in 0.5wt.% NaCl solution acidified to pH 2.8 with acetic acid and then allowed to dry at ambient conditions for 1 hour before being placed in a humidity chamber set at 95% relative humidity (RH). The 4-minute immersion inoculation process is similar to the approach taken in previous studies (LeBozec et al., 2004). Two different exposure temperatures were used in this study, one set of panels exposed to 95% RH and 25°C, and the other set exposed to 95%RH and 70°C.

Analysis

Scribe creep measurements were made after 6 weeks exposure in the humidity chamber. A Keyence VHX2000 digital microscope was used to capture images of the corrosion-affected areas of the test panels after exposure. The lens was tilted at an angle of approximately 30-degrees to give a satisfactory image of any filiform or blistering of the painted surface. Imaging software was used to measure the filiform or blister area for each of the test panels and to stitch images to give a full scribe-length composite photomicrograph. Scanning electron microscopy (SEM) was performed with a JEOL 6610 SEM equipped with Oxford X-Max Energy Dispersive X-ray (EDX) detector operated at 20keV. The sample was cut transverse to the scribe, mounted in epoxy, ground and polished to a position that intersected a filament. The SEM was operated in back-scattered electron, (BSE), mode to distinguish clearly between substrate, corrosion product and coating phases, and to minimize charging effects. Elemental analysis of corrosion products and substrate phases was conducted using EDX.

RESULTS

Appearance of Exposed Test Panels

Exposed test panels developed different paint defects, see figure 1. Long, thin filaments extending from the scribe were observed for many of the test panels. Corrosion-affected area was calculated by summing the area of each paint defect for each panel, see example measurement in figure 1b. Paint blistering was also observed, typically directly adjacent to the scribe but also less frequently observed as a string of discrete blisters, see figure 1c. Cracking of the clearcoat layer above the blisters was also observed in figure 1c.

 ISBN: 978-1-926872-32-2

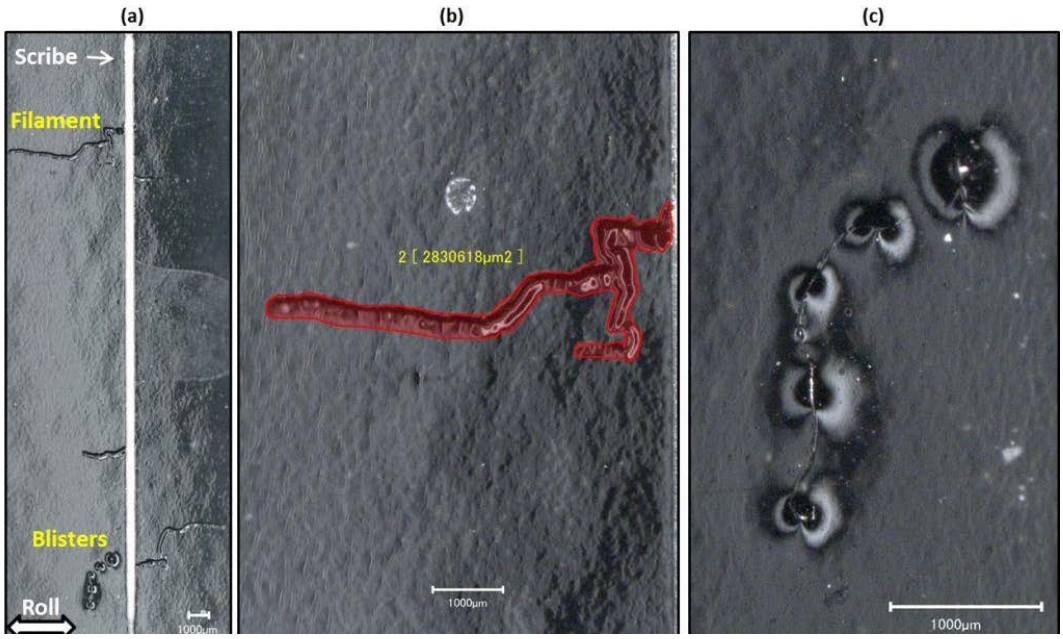

Figure 1 – paint defects induced on the scribed panels (AA6022 substrate, rolling direction perpendicular to scribe, 70°C exposure), (a) full panel view (stitched image), (b) detail view of filament and (c) detail view of blister string.

Filament growth in directions other than the rolling direction was observed although the overall trend showed filaments progressing parallel to the rolling direction, see figure 2.

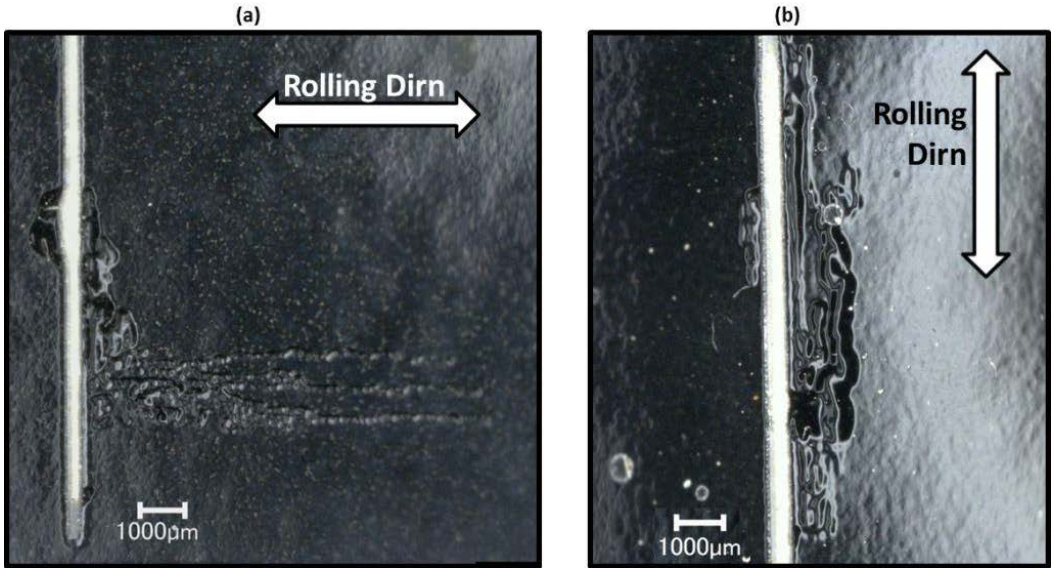

Figure 2 - Filiform growth in-line with rolling direction (AA6111 substrate, 70°C exposure)

Affected Area Measurements

The total corrosion-affected area for each panel was calculated by summing the area of each filament or blister for each panel and the results are presented as interaction plots in figure 3.

 ISBN: 978-1-926872-32-2

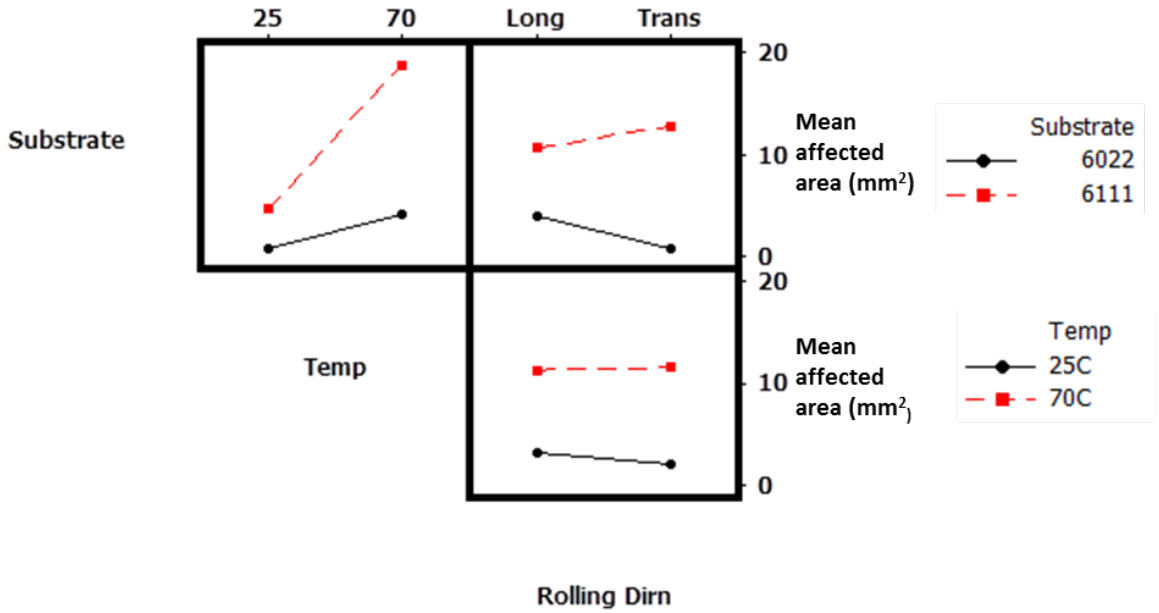

Figure 3 - Interactions and main effects plots for mean corrosion-affected area for the two substrates, at low and elevated exposure temperatures and in different rolling directions.

The high-copper alloy AA6111 substrate panels developed greater corrosion-affected areas than the low-copper alloy AA6022 under all test conditions. The steep slope for the mean values of affected area following room temperature and elevated temperature exposures (refer to upper left hand box of figure 3) show that the exposure temperature was the most significant factor for corrosion propagation on AA6111 substrate. Enhanced corrosion at higher temperature was also indicated but not as pronounced for AA6022 substrate. Greater total corrosion-affected area was measured on AA6111 panels with scribes cut parallel to the rolling direction (transverse). The opposite effect was observed for AA6022.

The effect of exposure temperature on the corrosion activity for each substrate is shown in detail in figure 4. Increased corrosion activities for AA6111 compared to AA6022 and the sharp effect of exposure temperature on the total affected area for AA6111 are clear from the boxplots.

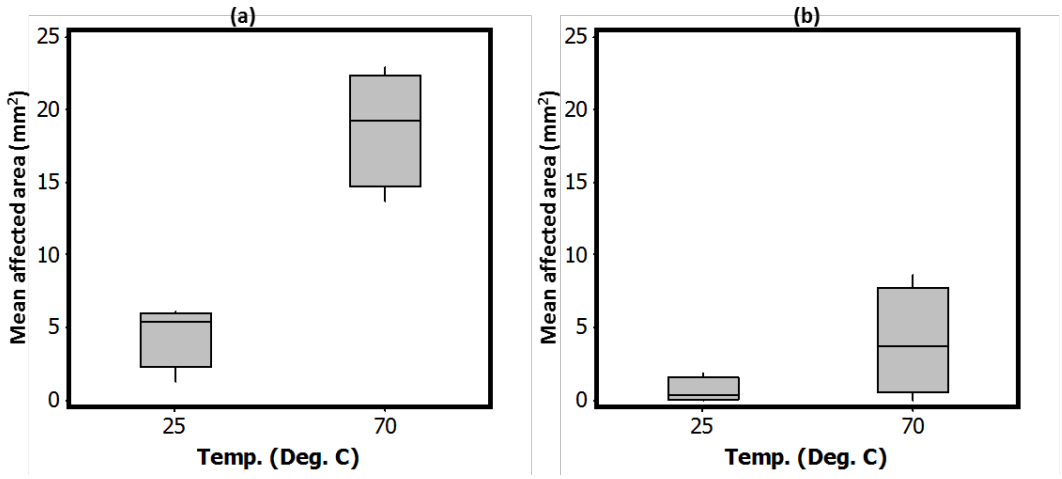

Figure 4 - Boxplots of affected area at 25°C and 70°C exposures for (a) AA6111 and (b) AA6022 substrates

 ISBN: 978-1-926872-32-2

Cross-Sectional Analysis

Figure 5 shows the surface and cross-section of an AA6022 test panel exposed at the 70°C temperature. Cross-sectional analysis showed the presence of dense corrosion products within the filament, see figure 5c, which displaced the e-coat layer. Cracks in the corrosion products are likely due to dehydration after removal of the test panel from the humidity chamber. The corrosion products form a wedge, exerting a prying force on the overlying coatings. Evidence of corrosion progression in to the substrate is also seen in figure 5c and at higher magnification in figure 6a. The progression of corrosion attack in to the substrate thickness is via grain boundaries, known as inter-granular corrosion, IGC.

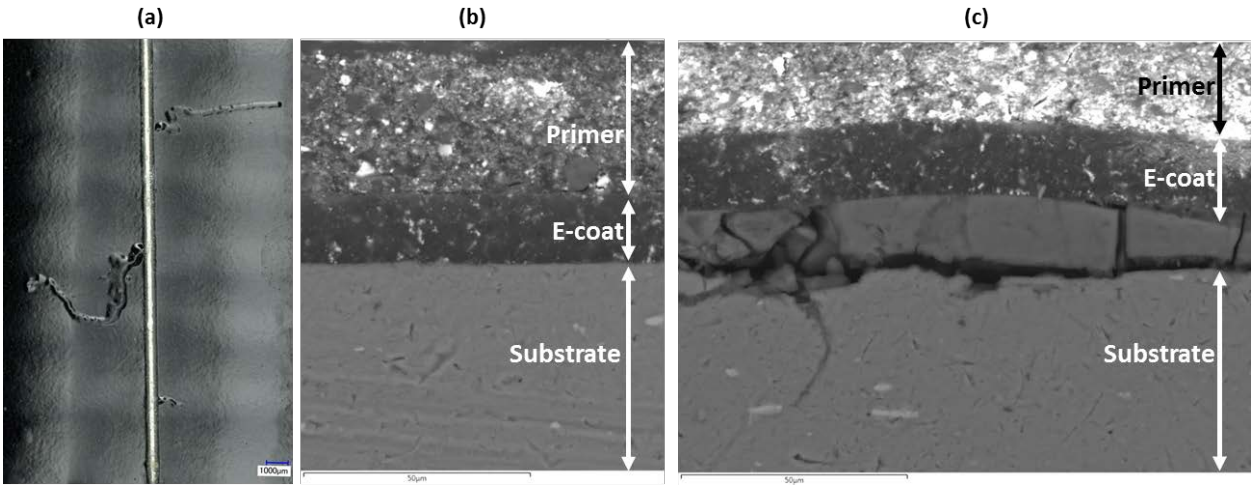

Figure 5 – AA6022 panel exposed at 70C (a) surface view, (b) BSE micrograph of cross section at an unaffected area and (c) BSE micrograph through filament.

 ISBN: 978-1-926872-32-2

EDX analysis was used to compare the elemental composition within the substrate to the composition of the corrosion products. The scanning area for the corrosion product is outlined in figure 6a. The substrate spectrum and composition is given in figure 6b and the corrosion product analysis is given in figure 6c. As expected, the substrate composition was dominated by the aluminum content (95 weight percent, wt.%), with several of the alloying elements also detected (refer to table 1). The corrosion product was almost 60wt.% oxygen, and approximately 40wt.% aluminum. Small quantities of chlorine, 0.2wt.%, and sulphur, 0.1wt.%, were also detected in the corrosion product scanned area.

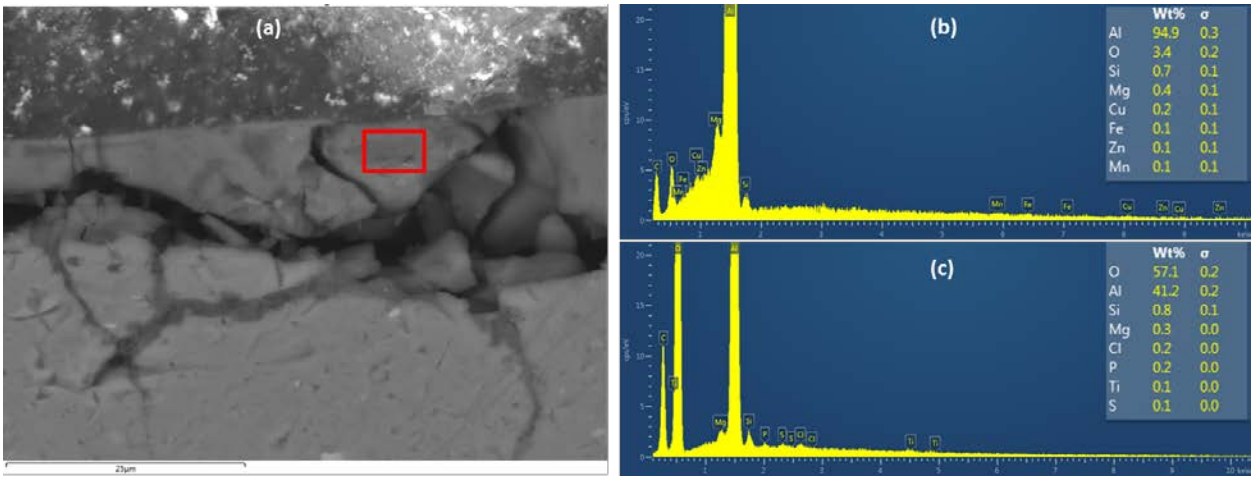

Figure 6 - Micrograph of filament cross-section (a) detail view of corrosion products and IGC, (b) EDX analysis of the substrate and (c) EDX analysis of the corrosion product at the region denoted by the red box in (a).

DISCUSSION

Effect of Substrate

The main compositional difference between the two substrates tested in this work is the copper concentration; AA6111 was measured with average 0.5wt.% Cu compared to AA6022 with average 0.1wt.% Cu. The other alloying elements are within 0.1% for the two substrates, refer to table 1. Enhancement of localized corrosion of aluminum alloys due to the presence of copper has been reported previously (Liang et al., 2013; Szklarska-Smialowska, 1999) and so the increased affected area measurements for AA6111 compared to AA6022 presented in figure 3 is attributed to the relatively higher copper content in the former. As discussed in the introduction, copper-rich IMPs are understood to act as local cathodes, promoting corrosion of adjacent anodic areas via galvanic action.

EDX analysis of the corrosion products inside the filament show high levels of oxygen compared to the substrate. The ratio of oxygen to aluminum was approximately 3:2 (57wt.% O, 41wt.% Al), suggesting the possibility of the corrosion product comprising essentially Al_2O_3. Small amounts, 0.2wt.% and 0.1wt.% respectively, of the corroding species chloride and sulphur were also detected within the corrosion product. Presence of chlorine towards the head of the filament supports the classic filiform corrosion model described by Delplancke et al. (2001) and LeBozec et al. (2004).

The effects of the substrate composition on the overlaying paint layers and the interface between the substrate and the paint layers must also be considered. Zinc-phosphate conversion coating deposits at different rates

 ISBN: 978-1-926872-32-2

across the electrochemically-varying surface, with negligible coating deposition on a cathodic site, such as copper-rich phases. The copper-rich sites can therefore be considered to be weak points in the substrate to coating interface. The increased number, density and, possibly, size of copper-rich IMPs at the AA6111 surface compared to the AA6022 therefore act to enhance underpaint corrosion activity both via a galvanic action and as sites of poorly-adhering coatings.

Effect of Rolling Direction

Filaments and blisters were observed to align generally parallel to the rolling direction, see figure 2. This means that corrosion activity for transverse panels, where the scribe was parallel to the rolling direction, tended to cluster and propagate directly adjacent to the scribed area whereas the longitudinal panels tended to develop filaments that extended perpendicular to the scribe and therefore propagated away from the scribe. Alignment of filament growth with rolling direction has been reported previously for 6016 aluminum alloy after the classic HCl-vapor inoculation and 80%RH, 40°C exposure period (X. F. Liu, 2007). This difference in filament direction is of course significant for quantification of filiform corrosion, typically measured as the extent of the filament perpendicular to the scribe. It should be necessary to state in each case whether the scribe is parallel or perpendicular to the substrate rolling direction.

The scribe orientation might also be significant for the filiform corrosion propagation rate and mechanism, given the relative proximity of the transverse filament heads to the defect (scribed) area compared to the longitudinal scenario. This is perhaps exemplified in figure 2a where the affected area adjacent to the scribe appears to be rather grossly blistered whereas the long filaments propagating away from the scribe are relatively fine and non-protruding. This appears to be in line with the suggestion from Delplancke et al. (2001) that access of oxygen to the filament head can reduce the classic filiform corrosion activity. It does not however necessarily guarantee the arrest of all under-film corrosion, as noted by the significant affected-area measurements for transverse panels in figure 3.

The data in figure 3 also suggest that the two substrates respond differently to the scribe orientation, with AA6111 developing higher corrosion activity on panels scribed parallel to the rolling direction and AA6022 developing higher corrosion activity on panels scribed perpendicular to the rolling direction. Given the overall increased corrosion rate for AA6111 relative to AA6022 under the test conditions here, it may be possible that the corrosion initiation is reduced for transverse panels but the propagation rates are higher than the longitudinal panels. The longitudinal panels, with greater likelihood of IMPs intersecting the scribe line, have a greater number of potential initiation sites than the transverse panels. The transverse panels have a shorter path between the active filament head and the driving cathodic tail. Taking the sum of these rolling direction effects for both substrates masks the differences, as indicated by the approximately flat lines connecting mean affected area values for rolling directions at each exposure temperature, see lower right-hand box in figure 3.

Effect of Exposure Temperature

Exposure at 70°C rather than 25°C for a given humidity level (95%RH) provoked a dramatic increase in the magnitude of corrosion-affected area for painted AA6111 panels. The low-copper substrate, AA6022, also developed increased corrosion-affected area at the higher exposure temperature, although some overlap of the measured affected areas at the two exposure temperatures is shown in figure 4b. It is not clear from the testing to date whether this reduced affect for AA6022 was due to an overall slower reaction or possibly a self-limiting effect for AA6022.

The higher-temperature exposure was intended to push the paint layers outside the conventional test parameters. Environmental conditions of 70°C and 95%RH are likely near or above the Tg of the coating layers, with the possible exception of the e-coat layer, which has been reported to have a Tg value around 80°C (Romano, Olivier, Vandermiers, & Poelman, 2006). That Tg value might be effectively reduced in the high-humidity

 ISBN: 978-1-926872-32-2

environment used in this work. In any case, it is expected that the effectiveness of the paint coatings as barriers to water and oxygen ingress was significantly reduced under the higher temperature exposure. The results of this study support previous reports that water uptake rates did not have a significant effect on filiform corrosion (Delplancke et al., 2001; Prosek et al., 2012); if the water uptake rate was a very significant factor, then the higher temperature exposure would be expected to lead to greatly-enhanced corrosion-affected area for all the 70°C test panels but the substrate type was the more significant factor, see figures 3-4. Clearly the elevated temperature exposure did provoke increased corrosion activity than the lower exposure temperature, however, the effective filiform corrosion resistance is a function of the response of the substrate to coating interface to the environment, rather than a function of the amount of moisture delivered to the corroding surface.

Evidence of inter-granular corrosion, IGC, progressing into the substrate was seen on the cross-section of the filament examined in figure 6a. The occurrence of IGC highlights the necessity to consider different corrosion mechanisms and reactions occurring during the exposure period. The various blistering and filiform corrosion morphologies observed in figure 1 also indicate that consideration of a single response type for a given substrate and coating system is too simplistic a model for aluminum automotive body panels. Further research is necessary to develop a comprehensive model of under-paint corrosion activity for such panels.

CONCLUSIONS

- Increased concentration of copper in the aluminum alloy composition led to a significant reduction in filiform corrosion resistance of the painted panel.
- Environmental exposure at higher temperature, 70°C versus 25°C, provoked strongly-increased corrosion activity for the copper-containing aluminum alloy at a given humidity level.
- Rolling direction had a clear effect on the direction of filiform and blister growth but further study is required to clarify whether difference mechanisms occur for panels scribed perpendicular and parallel to the rolling direction.
- Under-paint corrosion activity for aluminum automotive panels is the response of a complex system to the test or service environment.

REFERENCES

Afseth, A., Nordlien, J. H., Scamans, G. M., & Nisancioglu, K. (2002). Effect of thermo-mechanical processing on filiform corrosion of aluminium alloy AA3005. *Corrosion Science, 44*(11), 2491-2506. doi: http://dx.doi.org/10.1016/S0010-938X(02)00036-7

Bautista, A. (1996). Filiform corrosion in polymer-coated metals. *Progress in Organic Coatings, 28*(1), 49-58. doi: http://dx.doi.org/10.1016/0300-9440(95)00555-2

Bovard, F. S. S., Kevin A.; Courval, Gregory J.; McCune, Duncan; Jafolla, Tracie; Tardiff, Janice L.; Ramamurthy, Sridhar; Singleton, Raymund. (2010). *Cosmetic Corrosion Test for Aluminum Autobody Panels: Final Report*. Paper presented at the SAE 2010 World Congress, Detroit, Michigan, USA.

Davoodi, A., Pan, J., Leygraf, C., & Norgren, S. (2008). The Role of Intermetallic Particles in Localized Corrosion of an Aluminum Alloy Studied by SKPFM and Integrated AFM/SECM. *Journal of the Electrochemical Society, 155*(5), C211-C218. doi: 10.1149/1.2883737

Delplancke, J. L., Berger, S., Lefèbvre, X., Maetens, D., Pourbaix, A., & Heymans, N. (2001). Filiform corrosion: interactions between electrochemistry and mechanical properties of the paints. *Progress in Organic Coatings, 43*(1–3), 64-74. doi: http://dx.doi.org/10.1016/S0300-9440(01)00216-8

Guillaumin, V., & Mankowski, G. (2000). Localized corrosion of 6056 T6 aluminium alloy in chloride media. *Corrosion Science, 42*(1), 105-125. doi: http://dx.doi.org/10.1016/S0010-938X(99)00053-0

Jenkins, A. T. A., & Armstrong, R. D. (1996). The breakdown in the barrier properties of organic coatings due to filiform corrosion. *Corrosion Science, 38*(7), 1147-1157. doi: http://dx.doi.org/10.1016/0010-938X(96)00009-1

Jiang, L., Wolpers, M., Volovitch, P., & Ogle, K. (2012). The degradation of phosphate conversion coatings by electrochemically generated hydroxide. *Corrosion Science, 55*(0), 76-89. doi: http://dx.doi.org/10.1016/j.corsci.2011.10.004

Kaesche, H. (1978). Passivity and Breakdown of Passivity of Aluminum in Aqueous Electrolytes *Passivity of metals* (pp. 935-959). United States: Electrochemical Society, Inc.

LeBozec, N., Persson, D., & Thierry, D. (2004). In Situ Studies of the Initiation and Propagation of Filiform Corrosion on Aluminum. *Journal of the Electrochemical Society, 151*(7), B440-B445. doi: 10.1149/1.1760577

Liang, W. J., Rometsch, P. A., Cao, L. F., & Birbilis, N. (2013). General aspects related to the corrosion of 6xxx series aluminium alloys: Exploring the influence of Mg/Si ratio and Cu. *Corrosion Science, 76*(0), 119-128. doi: http://dx.doi.org/10.1016/j.corsci.2013.06.035

Liu, X. F. (2007). Filiform corrosion attack on pretreated aluminum alloy with tailored surface of epoxy coating. *Corrosion Science, 49*(9), 3494-3513. doi: http://dx.doi.org/10.1016/j.corsci.2007.03.031

Liu, Y., Zhou, X., Thompson, G. E., Hashimoto, T., Scamans, G. M., & Afseth, A. (2007). Precipitation in an AA6111 aluminium alloy and cosmetic corrosion. *Acta Materialia, 55*(1), 353-360. doi: http://dx.doi.org/10.1016/j.actamat.2006.08.025

McMurray, H. N., Holder, A., Williams, G., Scamans, G. M., & Coleman, A. J. (2010). The kinetics and mechanisms of filiform corrosion on aluminium alloy AA6111. *Electrochimica Acta, 55*(27), 7843-7852. doi: http://dx.doi.org/10.1016/j.electacta.2010.04.035

Nichols, M. E., & Darr, C. A. (1998). Effect of weathering on the stress distribution and mechanical performance of automotive paint systems. *Journal of Coatings Technology, 70*(885), 141-149.

Ogle, K., Tomandl, A., Meddahi, N., & Wolpers, M. (2004). The alkaline stability of phosphate coatings I: ICP atomic emission spectroelectrochemistry. *Corrosion Science, 46*(4), 979-995. doi: http://dx.doi.org/10.1016/S0010-938X(03)00182-3

Olivier, M. G., Poelman, M., Demuynck, M., & Petitjean, J. P. (2005). EIS evaluation of the filiform corrosion of aluminium coated by a cataphoretic paint. *Progress in Organic Coatings, 52*(4), 263-270. doi: http://dx.doi.org/10.1016/j.porgcoat.2004.05.008

Perera, D. Y., & Vanden Eynde, D. (1987). Moisture and temperature induced stresses (hygrothermal stresses) in organic coatings. *Journal of Coatings Technology, 59*(748), 55-63.

Prosek, T., Nazarov, A., Olivier, M.-G., Vandermiers, C., Koberg, D., & Thierry, D. (2010). The role of stress and topcoat properties in blistering of coil-coated materials. *Progress in Organic Coatings, 68*(4), 328-333. doi: http://dx.doi.org/10.1016/j.porgcoat.2010.03.003

Prosek, T., Nazarov, A., Stoulil, J., & Thierry, D. (2012). Evaluation of the tendency of coil-coated materials to blistering: Field exposure, accelerated tests and electrochemical measurements. *Corrosion Science, 61*(0), 92-100. doi: http://dx.doi.org/10.1016/j.corsci.2012.04.026

Romano, A. P., Olivier, M. G., Vandermiers, C., & Poelman, M. (2006). Influence of the curing temperature of a cataphoretic coating on the development of filiform corrosion of aluminium. *Progress in Organic Coatings, 57*(4), 400-407. doi: http://dx.doi.org/10.1016/j.porgcoat.2006.09.024

Simões, A., Battocchi, D., Tallman, D., & Bierwagen, G. (2008). Assessment of the corrosion protection of aluminium substrates by a Mg-rich primer: EIS, SVET and SECM study. *Progress in Organic Coatings, 63*(3), 260-266. doi: 10.1016/j.porgcoat.2008.02.007

Sun, X., Susac, D., Li, R., Wong, K. C., Foster, T., & Mitchell, K. A. R. (2002). Some observations for effects of copper on zinc phosphate conversion coatings on aluminum surfaces. *Surface and Coatings Technology, 155*(1), 46-50. doi: http://dx.doi.org/10.1016/S0257-8972(02)00027-0

Susac, D., Sun, X., Li, R. Y., Wong, K. C., Wong, P. C., Mitchell, K. A. R., & Champaneria, R. (2004). Microstructural effects on the initiation of zinc phosphate coatings on 2024-T3 aluminum alloy. *Applied Surface Science, 239*(1), 45-59. doi: http://dx.doi.org/10.1016/j.apsusc.2004.04.038

Szklarska-Smialowska, Z. (1999). Pitting corrosion of aluminum. *Corrosion Science, 41*(9), 1743-1767. doi: http://dx.doi.org/10.1016/S0010-938X(99)00012-8